

Continuum excitations of ^{26}O in a three-body model: 0^+ and 2^+ states

L. V. Grigorenko^{1,2,3} and M. V. Zhukov⁴¹*Flerov Laboratory of Nuclear Reactions, JINR, Dubna RU-141980, Russia*²*National Research Nuclear University "MEPhI", Kashirskoye shosse 31, RU-115409 Moscow, Russia*³*National Research Centre "Kurchatov Institute", Kurchatov sq. 1, RU-123182 Moscow, Russia*⁴*Fundamental Physics, Chalmers University of Technology, S-41296 Göteborg, Sweden*

(Received 11 March 2015; revised manuscript received 18 May 2015; published 25 June 2015)

The structure and decay dynamics for 0^+ and 2^+ continuum excitations of ^{26}O are investigated in a three-body $^{24}\text{O}+n+n$ model. The validity of a simple approximation for the cross section profile for long-lived $2n$ emission is demonstrated. A sequence of three 0^+ monopole ("breathing mode" type) excited states is predicted. These states could probably be interpreted as analogs of Efimov states pushed in the continuum due to insufficient binding. The calculated energies of the 2^+ states are related to the excitation spectrum of ^{25}O . We discuss the correlation between the predicted ^{26}O spectrum and experimental observations.

DOI: [10.1103/PhysRevC.91.064617](https://doi.org/10.1103/PhysRevC.91.064617)

PACS number(s): 21.60.Gx, 21.10.Tg, 21.45.-v, 24.50.+g

I. INTRODUCTION

The interest in extremely heavy oxygen isotopes is very high today, see Refs. [1–5]. One of the strongest motivations emanates from the structure theory [6–9]. The evolution of binding energies along the oxygen isotopic chain appears to be highly sensitive to the details of interactions and procedures used in the modern structure approaches thus providing a stringent test for their quality. This field of research concentrates on the short distances and short-range correlations. Recently it has been demonstrated that another source of inspiration here can be connected to the continuum properties of these systems and, correspondingly, to the long-range correlations [6,10–13].

The question of prospects to search for neutron radioactivity has been considered in Ref. [10]. In contrast to at the proton dripline, characterized by large Coulomb barriers, in the vicinity of the neutron dripline, the emission of neutrons from the particle-unstable ground state (g.s.) can be hindered mainly by centrifugal barriers (we do not consider the possible structural hindrance factors, connected with many-body effects for the ground state neutron emitters). For isotopes with an odd number of neutrons such barriers appear to be sufficient to produce long-lived (radioactivity lifetime scale) ground states only beyond the s - d shell. Discussion of such a remote region of the dripline is not of a practical importance nowadays. However, a more complicated phenomenon comes into play for the particle-unstable dripline systems with an even number of neutrons. The pairing interaction can produce specific decay energy conditions which force a simultaneous emission of two (or even four) neutrons. The level schemes for ^{26}O and ^{25}O illustrating this situation are given in Fig. 1. These, so-called true three-body (five-body) decays, are affected by the hindrance factor connected with an appearance of specific additional barriers in the few-body dynamics [see the discussion around Eq. (3) below]. Thus the search for novel types of a radioactivity phenomena, namely, two- and four-neutron radioactivities, becomes prospective.

Among the realistic candidates for $2n$ and $4n$ radioactivity search ^{26}O and ^{28}O were considered in Ref. [10]. Since that time a hint for the very long lifetime ($T_{1/2} = 4.5_{-1.5}^{+1.1}$ ps) was obtained for ^{26}O in Ref. [3]. Improved theoretical

lifetime estimates in Ref. [11] indicated that an extremely low three-body (total) decay energy, $E_T < 1$ keV, is required to produce such a long lifetime. A realization of such a small decay energy in the nature seems unrealistic, however, the experimental decay energy E_T limit for ^{26}O g.s. was steadily decreasing towards zero in recent years. At MSU the value $E_T = 150_{-150}^{+50}$ keV was obtained [2]. At GSI $E_T < 120$ keV or $E_T < 40$ keV was found depending on confidence level 95% or 68%, which was chosen for the analysis [4]. In RIKEN, ^{26}O and ^{25}O were also produced from ^{27}F and ^{26}F beams [5], with much higher statistics than in Refs. [2–4]. Their preliminary data also showed the ground state just above the $^{24}\text{O}+2n$ threshold, in addition to the newly observed excited state at little over 1 MeV. It should be noted that very small decay energy ($E_T \sim 20$ keV) was predicted theoretically in Ref. [6]. Thus, really extreme low decay energy of this nucleus cannot be excluded.

In recent years there were important advances in the studies of the lightest $2p$ emitter ^6Be [14–18]. Considering also the long history of studies of the $2n$ halo system ^6He in a three-cluster $\alpha+n+n$ approximation [19–23], it can be concluded that the understanding of the three-body dynamics in p -shell nuclei is reasonably developed. In contrast, for s - d shell systems the situation is much less advanced. Only very recently interesting results were obtained for the two-proton emitter ^{16}Ne [24,25]. The continuum three-body dynamics of the neutron-rich s - d shell nuclei also remains poorly investigated with just a few examples of such studies [6,11–13], elaborating mainly the ground state properties.

In previous works on ^{26}O [10,11] we concentrated on the decay studies of the g.s. in quite schematic approaches aiming first of all at a qualitative understanding of the underlying physics for long-living neutron emitters. In this work we consider the population and decays of the ^{26}O 0^+ and 2^+ continuum states using more realistic model assumptions, in a broad energy range, and with more details provided. In this work we report several nontrivial results concerning the three-body continuum dynamics of the s - d shell nuclei by the example of ^{26}O , which provides us important general insights in this question. Among the obtained results are (i) the validity

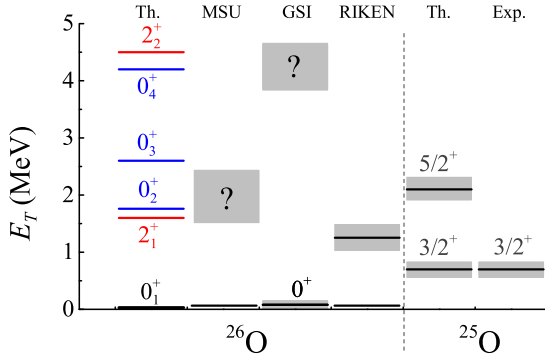


FIG. 1. (Color online) Experimentally observed energy levels of ^{26}O [3–5] and ^{25}O . For theory results the level scheme predicted for ^{26}O is shown which is based on the one assumed for ^{25}O .

of the simple approximation to the spectrum shape in the case of radioactive $2n$ decay, (ii) the existence of extreme peripheral 0^+ monopole excitations in the low-lying spectrum of ^{26}O .

II. THEORETICAL MODEL

The model applied to ^{26}O in this work generally follows the approach of Ref. [11]. To provide reasonable predictions concerning the excitation spectrum of ^{26}O the improvements concerning the reaction mechanism treatment were implemented, see, e.g., [16,25]. For some direct reactions the problem of population and decay of three-body states can be formulated in terms of the three-body inhomogeneous Schrödinger equation

$$(\hat{H}_3 - E_T)\Psi_{E_T}^{(+)} = \Phi_{\mathbf{q}},$$

$$\hat{H}_3 = \hat{T}_3 + V_{n_1-n_2} + V_{\text{core-}n_1} + V_{\text{core-}n_2} + V_3(\rho),$$

with the source function $\Phi_{\mathbf{q}}$ depending only on one parameter connected to the reaction mechanism: the transferred momentum \mathbf{q} . The dynamics of the three-body $^{24}\text{O}+n+n$ continuum of ^{26}O is described by the wave function (WF) $\Psi^{(+)}$ with pure outgoing asymptotic in the hyperspherical harmonics (HH) formalism:

$$\Psi_{E_T}^{JM_J(+)} = \rho^{-5/2} \sum_{K\gamma} \chi_{K\gamma}^{(+)}(\rho) \mathcal{J}_{K\gamma}^{JM_J}(\Omega_\rho),$$

$$\chi_{K\gamma}^{(+)}(\rho) \stackrel{\rho \rightarrow \infty}{\sim} \mathcal{H}_{K+3/2}^{(+)}(\chi\rho) \sim \exp(+i\chi\rho), \quad (1)$$

where \mathcal{H} denote the Riccati-Bessel functions of half-integer index and the “multi-index” γ denotes the complete set of quantum numbers except for the principal quantum number K : $\gamma = \{L, S, l_x, l_y\}$.

The three-body calculations in the HH method utilize the transition from the three-body Jacobi coordinates $\{\mathbf{x}, \mathbf{y}\} = \{x, \Omega_x, y, \Omega_y\}$ to the collective coordinates $\{\rho, \Omega_\rho\} = \{\rho, \theta_\rho, \Omega_x, \Omega_y\}$. The hyper-radius ρ (describing collective radial motion) and the hyperangle θ_ρ (responsible for geometry of the system at given ρ) are defined via the cluster

coordinates \mathbf{r}_i as

$$\mathbf{x} = \sqrt{\frac{A_1 A_2}{A_1 + A_2}} (\mathbf{r}_1 - \mathbf{r}_2),$$

$$\mathbf{y} = \sqrt{\frac{(A_1 + A_2) A_3}{A_1 + A_2 + A_3}} \left(\frac{A_1 \mathbf{r}_1 + A_2 \mathbf{r}_2}{A_1 + A_2} - \mathbf{r}_3 \right),$$

$$\rho = \sqrt{x^2 + y^2}, \quad \theta_\rho = \arctan(x/y). \quad (2)$$

Hypermomentum $\kappa = \sqrt{2ME_T}$ is the dynamic variable conjugated to hyper-radius. The mass M is an average nucleon mass for the considered nucleus.

The hyperspherical harmonics $\mathcal{J}_{K\gamma}^{JM_J}$ with definite total angular momentum J and its projection M_J

$$\mathcal{J}_{K\gamma}^{JM_J}(\Omega_\rho) = \psi_L^{l_x l_y}(\theta_\rho) [[Y_{l_x}(\Omega_x) \otimes Y_{l_y}(\Omega_y)]_L \otimes X_S]_{JM_J}$$

form a full set of orthogonal functions on the five-dimensional “hypersphere” Ω_ρ . The pure hyperangular functions $\psi_L^{l_x l_y}$ are expressed in terms of Jacobi polynomials.

The three-body Schrödinger equation (1) in the hyperspherical basis is reduced to the set of coupled differential equations for the functions $\chi^{(+)}$:

$$\left[\frac{d^2}{d\rho^2} - \frac{\mathcal{L}(\mathcal{L}+1)}{\rho^2} + 2M\{E - V_{K\gamma, K\gamma}(\rho)\} \right] \chi_{K\gamma}^{(+)}(\rho)$$

$$= 2M \sum_{K'\gamma' \neq K\gamma} V_{K\gamma, K'\gamma'}(\rho) \chi_{K'\gamma'}^{(+)}(\rho) - 2M \Phi_{\mathbf{q}, K\gamma}(\rho), \quad (3)$$

which can be interpreted as motion of a single “effective” particle in a strongly deformed field. The “three-body potentials” (matrix elements of the pairwise potentials) $V_{K\gamma, K'\gamma'}(\rho)$ and the partial source terms $\Phi_{\mathbf{q}, K\gamma}$ are defined as

$$V_{K\gamma, K'\gamma'}(\rho) = \int d\Omega_\rho \mathcal{J}_{K'\gamma'}^{JM_J*}(\Omega_\rho) \sum_{i < j} V_{ij}(\mathbf{r}_{ij}) \mathcal{J}_{K\gamma}^{JM_J}(\Omega_\rho),$$

$$\Phi_{\mathbf{q}, K\gamma}(\rho) = \int d\Omega_\rho \mathcal{J}_{K'\gamma'}^{JM_J*}(\Omega_\rho) \Phi_{\mathbf{q}}(\rho, \Omega_\rho).$$

The details of the hyperspherical method application to various three-body systems in different physical situations can be found in the papers [15,19,26–28].

The important qualitative difference between Eq. (3) and the conventional two-body situation is that the “effective angular momentum” $\mathcal{L} = K + 3/2$ in the three-body problem is not equal to zero even for the lowest possible quantum state with $K = 0$. Thus, there exists a three-body centrifugal barrier even for decays via s -wave emission of neutral particles producing strong hindrance factors for the widths of such low-energy decays.

The differential cross section is expressed via the flux j induced by the WF $\Psi^{(+)}$ on the remote five-dimensional surface Ω_ρ with $\rho = \rho_{\text{max}}$

$$\frac{d\sigma}{dE_T d\Omega_\rho} \sim j, \quad j = \langle \Psi_{E_T}^{(+)} | \hat{j} | \Psi_{E_T}^{(+)} \rangle \Big|_{\rho_{\text{max}}}$$

$$= \frac{1}{M} \text{Im} \left[\Psi_{E_T}^{(+)\dagger} \rho^{5/2} \frac{d}{d\rho} \rho^{5/2} \Psi_{E_T}^{(+)} \right] \Big|_{\rho_{\text{max}}}. \quad (4)$$

The approach with inhomogeneous Schrödinger equation (1) had previously been applied to two different direct reaction mechanisms (knockout and charge-exchange) populating the three-body continuum of the ^6Be [16–18], ^{10}He [29], and ^{16}Ne [24,25].

The source function $\Phi_{\mathbf{q}}$ for the 0^+ continuum was approximated assuming a sudden removal of a d -wave proton from ^{27}F

$$\Phi_{\mathbf{q}}^{(0^+)} = v_0 \int d^3 r_p e^{i\mathbf{q}\mathbf{r}_p} \langle \Psi_{24\text{O}} | \Psi_{27\text{F}} \rangle, \quad (5)$$

where \mathbf{r}_p is the radius-vector of the removed proton. The ^{27}F g.s. WF $\Psi_{27\text{F}}$ was obtained in a three-body $^{25}\text{F}+n+n$ cluster model and the technicalities of proton removal from the ^{25}F core of the ^{27}F nucleus are the same as in calculations of Ref. [29].

The source function $\Phi_{\mathbf{q}}$ for the 2^+ continuum cannot be easily evaluated by a simple proton removal model in the framework of three-body approach to structure of ^{27}F . Therefore, we use the source generated by additionally acting on the valence neutrons of the ^{27}F g.s. WF by the quadrupole operator:

$$\Phi_{\mathbf{q}}^{(2^+)} = v_2 \int d^3 r_n e^{i\mathbf{q}\mathbf{r}_n} \langle \Psi_{24\text{O}} | \sum_{i=1,2} r_i^2 Y_{2m_i}(\hat{r}_i) | \Psi_{27\text{F}} \rangle. \quad (6)$$

Expressions of this type typically arise in the direct reaction studies and seem to be sufficiently suited for exploratory studies of 2^+ excitations in the ^{26}O case. The approximation is the same as used in the recent paper [25].

The sudden removal approximation is not intended for absolute cross section calculations, and therefore the source strength coefficients v_i in Eqs. (5) and (6) are arbitrary values providing the source function the correct dimension of [energy/length $^{5/2}$].

III. POTENTIALS

In this work we employ for the nucleon-nucleon channel the quasirealistic potential from Ref. [30] including central, spin-orbit, tensor, and parity-splitting terms.

In the $^{24}\text{O}-n$ channel we used the potential from [11] characterized as “moderate repulsion in s and p waves”. This is a Woods-Saxon potential with radius $r_0 = 3.5$ fm, diffuseness $a = 0.75$ fm, and depth parameters $V_s = 70$ MeV and $V_p = 70$ MeV for s and p waves, respectively. The d -waves component was modified by an inclusion of the ls interaction to produce realistic excitation spectrum of ^{25}O : $V_d = -33$ MeV, $V_{ls} = -5$ MeV. We also varied the ls interaction to check the sensitivity to this parameter, see Secs. VI and VII.

The three-body potential $V_3(\rho)$ depending on ρ with the Woods-Saxon parametrization ($\rho_0 = 5$ fm, $a = 0.9$ fm) is used to control the decay energy E_T when the fine adjustment is needed, see the discussion in [31]. This potential is very small (on the level of just a few keV) for the $^{24}\text{O}-n$ potential chosen in this work and therefore V_3 does not influence the other results of the calculations on the practical level.

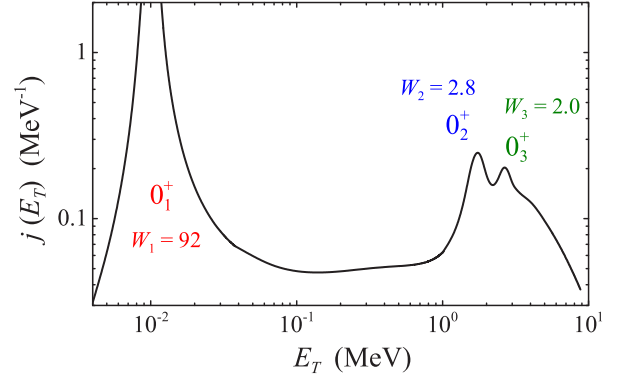


FIG. 2. (Color online) The 0^+ excitation spectrum of ^{26}O calculated by the three-body model for proton knockout from ^{27}F . Weights, W_i , of the peaks are shown in percent.

IV. EXCITATION SPECTRUM AND STRUCTURE OF 0^+ STATES

A calculated spectrum for 0^+ continuum states of ^{26}O is shown in Fig. 2. In this particular calculation the g.s. is obtained at $E_T = 10$ keV. Two more states are obtained at about 1.76 and 2.6 MeV. Some hint for a broad 0^+ state at about 4.2 MeV can also be seen. Within the simple reaction model used in this work the ground 0^+ state is populated with the relative intensity $W_1 \sim 92\%$ indicated in Fig. 2, while the excited 0^+ states are populated at a level of $W_{i>1} \sim 2-3\%$. It can be expected that in more complicated reaction scenario the source function $\Phi_{\mathbf{q}}$ should have smaller affinity to the ^{26}O ground state WF and we can expect up to $W_{i>1} \sim 5-15\%$ population rates for the excited 0^+ states. The relative population intensities above are calculated by integration of the strength function Fig. 2 in the range $[E_{3r}(i) - \Gamma(i), E_{3r}(i) + \Gamma(i)]$ around the energy $E_{3r}(i)$ of the i th resonance which width is $\Gamma(i)$.

V. R-MATRIX LIKE PHENOMENOLOGY

The ideas of using R -matrix type expressions for analysis of the three-body excitations and decays have been discussed occasionally in the literature [14,28,32] in quite a sketchy way. It is important to understand general validity and limits of applicability of such expressions for practical application as for theoretical estimates and as for phenomenological analysis of experimental data.

It can be shown that for the source function normalized at given \mathbf{q} value

$$\int d\rho \rho^5 d\Omega_\rho 2M |\Phi_{\mathbf{q}}(\rho, \Omega_\rho)|^2 = 1,$$

the energy profile of flux is provided by the expression

$$j(E_T) = W(E_{3r}) \frac{\pi}{2M^2} \frac{\Gamma_K(E_T)}{(E_T - E_{3r})^2 - \Gamma(E_{3r})^2/4},$$

$$\Gamma_K(E_T) = 2\gamma_{\text{WL}} \theta_{K\gamma}^2 \frac{(2/\pi)}{J_{K+2}^2(\kappa\rho_{\text{ch}}) + Y_{K+2}^2(\kappa\rho_{\text{ch}})}. \quad (7)$$

Here the hypermomentum $\kappa = \sqrt{2ME_{3r}}$ is defined at the three-body resonance energy E_{3r} , and the “Wigner limit”

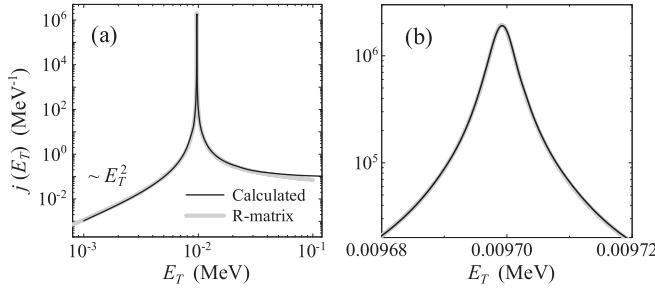


FIG. 3. Cross section profiles for the very narrow ^{26}O g.s. calculated by the three-body model and obtained by the R -matrix-type approximation are shown on two different scales in (a) and (b).

$\gamma_{\text{WL}} = 1/(2M\rho_{\text{ch}}^2)$ estimates the upper limit for the width. The functions J and Y are cylindrical Bessel functions regular and irregular at the origin, respectively. This expression is totally analogous to the standard two-body R -matrix expression as it is based on the assumption that the penetration in the three-body system is defined by the three-body channel in the hyperspherical decomposition of the WF with the lowest possible hypermomentum $R = K_{\text{min}}$. For systems with zero spin of the core the latter is trivially related to the total spin of the state: $K_{\text{min}} = J$. The “normalization” $W(E_{3r})$ is connected to the affinity of the source to the inner structure of the resonance; this value is expected to be smaller than unity, but of the order of unity for the realistic situation. It was found to be $W(\text{g.s.}) = 0.92$ in our calculations, see also Fig. 2.

The example of application of the R -matrix expression is provided in Fig. 3. The possibility of fitting the excitation profile by the Breit-Wigner shape in the vicinity of the resonance does not cause any doubts. However, it can be seen that the near-perfect description is provided by the R -matrix expression up to something like 10^5 widths away from the resonance. For this figure the “spectroscopic factor” $\theta_{K\gamma}^2$ is fitted in such a way that the calculated width Γ_K for the three-body resonance energy $E_{3r} = 9.7$ keV is exactly reproduced by the R -matrix expression [in this specific case $\Gamma_K(E_{3r}) = 4.04 \times 10^{-3}$ keV].

It is also necessary to fix one more parameter: the “channel radius” ρ_{ch} . In the three-body case this parameter does not have such a well-defined meaning as in two-body R -matrix phenomenology and some investigation is required here. Definition of the spectroscopic factor θ^2 for the single-channel approximation is

$$\theta_{K\gamma}^2(\rho_{\text{ch}}) = \frac{|\chi_{K\gamma}(\rho_{\text{ch}})|^2}{I(\rho_{\text{ch}})}, \quad I(\rho_{\text{ch}}) = \sum_{K\gamma} \int_0^1 dx |\chi_{K\gamma}(x\rho_{\text{ch}})|^2.$$

The θ^2 dependence on channel radius, obtained using the calculated three-body ^{26}O WF, is illustrated in Fig. 4. It is very stable in a broad range of channel radii, varying from 0.007 to 0.004 for $4 < \rho_{\text{ch}} < 25$ fm. The θ^2 variation for the mentioned range of channel radius is in very good agreement with the relative weight of the $[s^2]$ configuration calculated within the whole internal region $W(s^2) = 0.0067$, see also Table I. The calculated three-body width is reproduced for

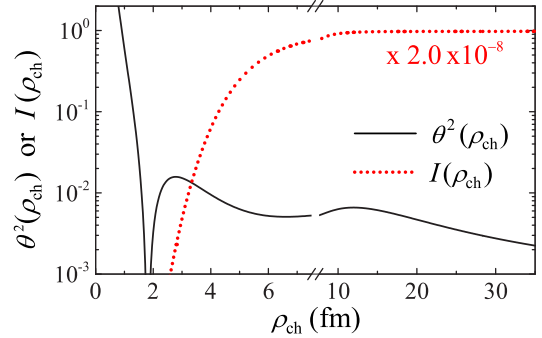


FIG. 4. (Color online) Spectroscopic factor θ^2 Eq. (7) as a function of channel radius ρ_{ch} . The dotted curve shows the dependence of the “internal normalization” I on ρ_{ch} .

$\rho_{\text{ch}} = 13$ fm and for less than $\pm 50\%$ variation of width we need to keep the channel radius in the range $9 < \rho_{\text{ch}} < 16$ fm.

We can see that the extension of a simple single channel R -matrix phenomenology, Eq. (7), to the three-body decays provides easily tractable and very reliable results for long-lived two-neutron emitters. We can also conclude that the use of typical R -matrix parameters, chosen according to the prescription discussed above, can be expected to provide widths values with an uncertainty around 50%, which is a quite accurate result for estimates concerning long-living states.

VI. THE MONOPOLE 0^+ EXCITATIONS

The nature of the excited 0^+ states is very interesting and deserves a special discussion. Table I provides the basic structure information about the ^{26}O 0^+ states indicating their high similarity. It is clear that a simple explanation for such a situation is that the predicted excited 0^+ states are all monopole (often called “breathing mode”) excitations.

To check this assumption we have studied the radial evolution and the correlation densities of the ^{26}O 0^+ WFs at corresponding energies. One can see in Fig. 5 that the g.s. WF density decreases more or less exponentially inside the barrier. At larger distances the behavior tends to be constant which corresponds to approaching the asymptotic behavior $\chi^{(+)} \sim \exp(+i\kappa\rho)$ of the three-body WF. However, for the 0_2^+ and 0_3^+ state WFs there exists one and two extra humps, respectively (indicated by arrows in Fig. 5), in the above-the-barrier slope of the density before the asymptotic

TABLE I. The three-body structure of the g.s. of initial ^{27}F nucleus and ^{26}O 0^+ excitations in terms of probability $W(l^2)$ in percent of the corresponding $[l_j^2]_0$ configuration. The energies of the states with respect to the three-body breakup threshold are provided in the last row.

l_j	^{27}F , g.s.	^{26}O , g.s.	^{26}O , 0_2^+	^{26}O , 0_3^+
$s_{1/2}$	0.55	0.67	3.7	3.8
$d_{3/2}$	84	79	80	86
$d_{5/2}$	13	19	6.0	6.1
E_T (MeV)	-3.2	0.01	1.7	2.6

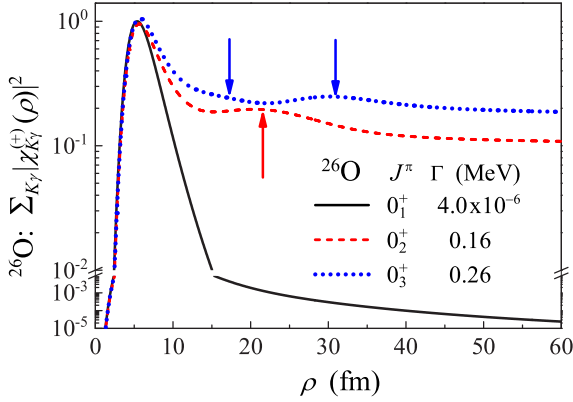


FIG. 5. (Color online) WF densities for the ^{26}O ground state and two excited 0^+ states. All WFs are normalized to unity maximum value. Arrows indicate the humps connected with monopole excitations.

(constant) behavior is achieved. This is exactly expected for the monopole states where the major WF component should have one or more nodes in the radial WF. The extreme radial extent of the humps is notable, e.g., the peak for 0_3^+ with $\rho \sim 30$ fm corresponds to typical single particle distances in the core-neutron channel of about 20 fm.

To understand the reasons for the monopole state formation we performed simple width estimates for major configurations of the ^{26}O WF. Figure 6 provides the estimates in a “direct decay” R -matrix model from Ref. [31]:

$$\Gamma_{j_1 j_2}(E_T) = \frac{E_T \langle V_3 \rangle^2}{2\pi} \int_0^1 d\varepsilon \frac{\Gamma_{j_1}(\varepsilon E_T)}{(\varepsilon E_T - E_{j_1})^2 + \Gamma_{j_1}(\varepsilon E_T)^2/4} \times \frac{\Gamma_{j_2}((1-\varepsilon)E_T)}{((1-\varepsilon)E_T - E_{j_2})^2 + \Gamma_{j_2}((1-\varepsilon)E_T)^2/4}. \quad (8)$$

This model approximates reasonably well the true three-body decay mechanism, and also provides a smooth transition to the sequential decay regime. The direct decay model is constructed in the spirit of independent particle approach with two nucleons being emitted from states with definite single-particle angular momenta j_1 and j_2 sharing the total decay

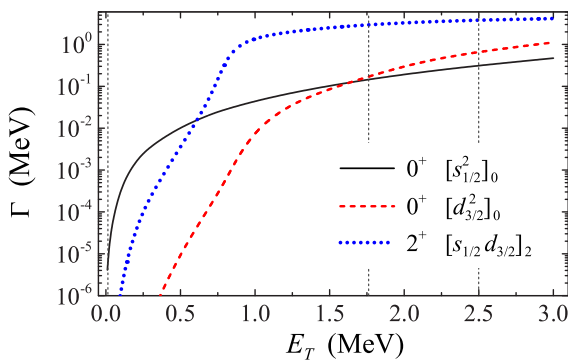


FIG. 6. (Color online) Width estimates for the 0^+ and 2^+ states of ^{26}O in the R -matrix-type approach of Eq. (8) for different $[j_1 j_2]_J$ configurations. Vertical dashed lines indicate the predicted positions of the 0^+ states.

energy E_T , but with interaction between nucleons neglected. The Γ_{j_i} is the standard R -matrix expression for the width as a function of the energy for the involved resonances in the $^{24}\text{O}+n$ subsystems. It is assumed that two-body resonant states with energies E_{j_i} are present in both two-body subsystems and that the values $\Gamma_{j_i}(E_{j_i})$ correctly describe their empirical widths. The matrix element $\langle V_3 \rangle$ can be well approximated as

$$\langle V_3 \rangle^2 = D_3 [(E_T - E_{j_1} - E_{j_2})^2 + (\Gamma_{j_1}(E_{j_1}) + \Gamma_{j_2}(E_{j_2}))^2/4],$$

where the parameter $D_3 \approx 1.0-1.5$ is a constant.

It can be seen in Fig. 6 that for low-energy decays of the 0^+ states the predominant contribution to the width is connected with the $[s_{1/2}^2]_0$ configuration of ^{26}O . Here the width associated with the dominant $[d_{3/2}^2]_0$ configuration of the WF (see Table I) is strongly suppressed. However, for $E_T > 0.77$ MeV the decay mechanism for the $[d_{3/2}^2]_0$ configuration changes to the sequential emission via the $d_{3/2}$ ground state of ^{25}O . So, at higher energies the partial width for this configuration rapidly grows and becomes approximately equal to that of the $[s_{1/2}^2]_0$ configuration at $E_T = 1.6$ MeV. This is approximately the energy at which the second 0^+ state appears. So, despite the simplicity of these estimates they provide a hint that the appearance of the excited 0^+ states could be connected with the ability of the $[d_{3/2}^2]_0$ configuration to propagate effectively to large distances above the barrier. We can estimate that the monopole states found are built on interference patterns between $[s_{1/2}^2]_0$ and $[d_{3/2}^2]_0$ components at large distances.

To get a deeper insight into the process we may investigate the three-body WF correlation densities, Fig. 7:

$$W(\rho, \theta_\rho) = \int d\Omega_x d\Omega_y |\Psi^{(+)}(\rho, \theta_\rho, \Omega_x, \Omega_y)|^2.$$

In the “Y” Jacobi system we should choose the mass number of the ^{24}O cluster as A_1 or A_2 in Eq. (2) and for such a relatively heavy core cluster we can approximate the distances between core and valence nucleons by

$$r_{\text{core-}n_1} = \sqrt{\frac{A_1 + A_2}{A_1 A_2}} \rho \sin(\theta_\rho),$$

$$r_{\text{core-}n_2} \approx \sqrt{\frac{A_1 + A_2 + A_3}{(A_1 + A_2) A_3}} \rho \cos(\theta_\rho).$$

Thus, the provided correlation densities illustrate the evolution of relative distances in the single-particle channels.

It can be seen in Fig. 7 that the correlation densities for the calculated 0_2^+ and 0_3^+ states have a complicated correlation pattern in the hyperangle θ_ρ at large distances $10 < \rho < 30$ fm. Such a triple-peak pattern should be connected with the important contribution of the $[d^2]$ configuration in the above-the-barrier region. The $[d^2]$ configuration is as expected dominant in the nuclear interior $\rho < 10$ fm, but for the ground state it is suppressed under the barrier, see Fig. 7(a). In contrast, for the 0_2^+ and 0_3^+ states, illustrated in Figs. 7(b) and 7(c), the $[d^2]$ component extends also to the peripheral region forming the triple-peak patterns.

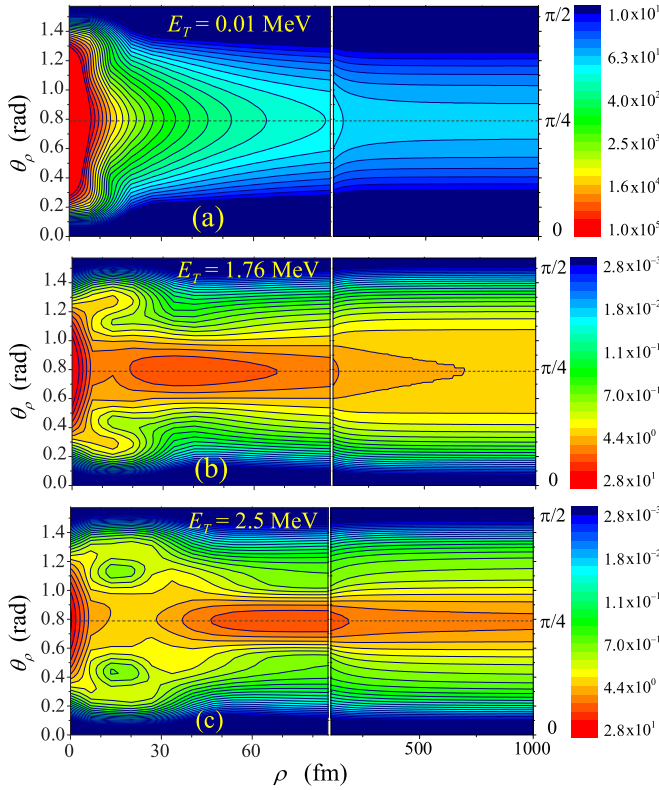


FIG. 7. (Color online) The ^{26}O WF correlation density $W(\rho, \theta_p)$ in the ‘‘Y’’ Jacobi system for the ground state (a) and two excited 0^+ states (b) and (c). Notice the change of ρ scale.

Figure 8 demonstrates the evolution of the 0^+ states with V_{ls} . This evolution provides some confirmation that the ‘‘remnants’’ of the broad monopole 0_4^+ state are present in the spectrum Fig. 2 at about 4 MeV. With V_{ls} approaching zero, the 0^+ spectrum shifts downwards in energy providing a much narrower, and thus well defined, 0_4^+ state. For larger negative V_{ls} values the 0_4^+ state increases in energy and is totally dissolved in the continuum.

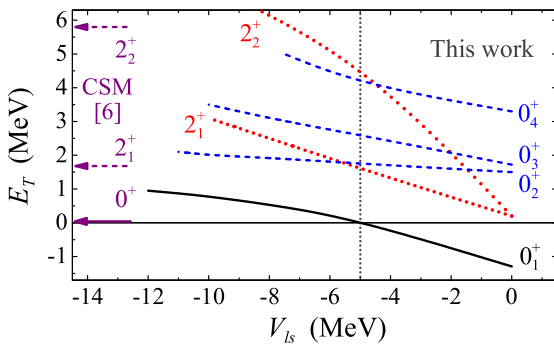


FIG. 8. (Color online) The systematics of the 0^+ and 2^+ states of ^{26}O as a function of the ls interaction intensity V_{ls} in the d -wave ^{24}O - n channel under the condition that the ^{25}O $d_{3/2}$ g.s. position remains fixed. The result for $V_{ls} = -5$ MeV (indicated by vertical dots) is provided in Fig. 1 as our main result. The predictions of Ref. [6] are indicated by arrows in the left part of the plot.

VII. THE 2^+ STATES

The excitation spectrum of ^{26}O is expected to have relatively low level density due to the simplicity of the spectrum of ^{25}O , where only one low-lying state is known so far ($d_{3/2}$ at 0.7 MeV). In the calculations we obtain just two 2^+ states where the lower one has a structure characterized by the configuration mixing $[d_{3/2}^2]_2 - [d_{5/2}^2]_2$, while the higher one is based on the $[s_{1/2}d_{3/2}]_2 - [s_{1/2}d_{5/2}]_2$ configurations. Within the three-body model the separation between these configurations is defined by the ls splitting between the ^{25}O g.s. $d_{3/2}$ and the yet unknown $d_{5/2}$ state. Figure 8 demonstrates the dependence of the positions of the 2^+ states on the intensity of the ls interaction under the condition that the ^{25}O $d_{3/2}$ g.s. position remains fixed. The 2^+ states naturally become degenerate for $V_{ls} = 0$.

Most of the calculations in this work are performed for $V_{ls} = -5$ MeV, which provides the position of the 0^+ g.s. to be exactly on the $2n$ threshold. Under this condition the predicted positions of the 2^+ state are 1.6 MeV and 4.5 MeV. The calculated three-body width value for the 2_1^+ state is $\Gamma = 115$ keV. However, the width of the states with an expected dominant sequential decay mechanism are not reliably predicted in the HH method calculations. For that reason we also performed estimates using the direct decay model expression Eq. (8). The result for the $[s_{1/2}d_{3/2}]_2$ configuration which has the most favorable penetration conditions is provided in Fig. 6. For the 2_1^+ state the value $\Gamma_{1/2,3/2} \approx 2.7$ MeV. However, it should be corrected for the weight of the $[s_{1/2}d_{3/2}]_2$ configuration in the interior of the three-body WF $\Psi^{(+)}$,

$$\Gamma = \Gamma_{j_1 j_2} W_{j_1 j_2}.$$

The value $W_{1/2,3/2} = 3.6\%$, which is quite small, is obtained in the three-body calculations. Then the estimate $\Gamma = 96$ keV is obtained. This value agrees well with the results of the three-body width calculations, and we estimate that it is realistic to expect the width of the first 2^+ state to be in the range 100–120 keV.

VIII. DISCUSSION OF THEORETICAL RESULTS ON ^{26}O SPECTRUM

In our calculations we have chosen the calculation scheme, where the effect of the occupied $d_{5/2}$ orbital in ^{25}O is imitated by inverse ls forces moving the $d_{5/2}$ state to an energy higher than that of the $d_{3/2}$ state. The particular value of this interaction was fixed by reproducing the near-threshold position of the ^{26}O g.s. Such a computation scheme is not free of problems, but it seems, however, to be quite successful for the ^{26}O nucleus. This nucleus is just two neutrons away from the ^{28}O neutron shell closure and the main dynamical degrees of freedom are connected just with the motion of the two valence nucleons. This is a clear motivation for the use of the three-body core+ n + n model.

The oxygen isotope chain was studied in details by Volya and Zelevinskiy [6] using the continuum shell model. They predicted the ^{26}O ground state position to be practically exactly on the threshold with $E_T = 21$ keV. Such a bold prediction was nicely confirmed by the recent experimental studies [2,4,5].

The predictions of [6] about 2^+ states are in reasonable agreement with our calculations: our 2_1^+ state position is around 100 keV lower in excitation energy than in Ref. [6] and, correspondingly, the 2_2^+ is about 1.7 MeV lower. The $0_{i>1}^+$ low-lying excited states are absent in the continuum shell model calculations of Ref. [6]. This, probably, could be connected to the “short range character” of the shell model calculations in general: in our calculations the excited 0^+ states require the dynamical range of tens of Fermi to be accounted for properly. Another possible reason could be that the treatment of the $^{24}\text{O}+n+n$ continuum in Ref. [6] is not fully dynamical, as it relies on the simplified three-body Green’s functions not including the N - N final-state interaction. For this reason it is astonishing that the width obtained in the current calculations practically coincides with results of Ref. [6]. According to our experience, the simplified three-body Green’s function should provide a width for the $[s^2]$ configuration decay which is ~ 10 – 30 times smaller than that obtained if appropriately taking the final state nucleon-nucleon interaction into account.

The ^{26}O g.s. was studied in [12]. The higher 0^+ excitations are not discussed in that work but there are some indications of the excited 0^+ at about 3.4 MeV, see, Fig. 1 of Ref. [12]. The authors do not elaborate this result and its reliability is not known; at least there is some indication of the possibility of an existence of the low-lying excited 0^+ in an alternative approach. The first 2^+ state was obtained at about $E_T = 1.35$ MeV in the recent calculations Ref. [13]. This value is not drastically different from our results and the results of [6].

The *ab initio* shell model theoretical calculations of Ref. [33] provided the excitation energy of the 2^+ state in ^{26}O in the range $E^* = 1.2$ – 1.7 MeV depending on the details of the calculations. The obtained results are reasonably consistent with other theoretical predictions.

IX. DISCUSSION OF RELEVANCE TO EXPERIMENTAL DATA

How could the predicted excitations of ^{26}O in our work be related to observations? The considerable evolution of the ^{26}O spectrum shape with the V_{ls} parameter is shown in Fig. 8. However, it should be noted that the predicted picture of *excitation energies* is relatively stable in this plot for reasonable variation of V_{ls} . In particular, the excitation energies for the $0_{i>1}^+$ states and 2_1^+ state are practically constant.

There is some evidence for intensity at about $E_T = 2$ MeV in Refs. [2,3]. A peak just above 1 MeV was observed in Ref. [5]. For this energy range we predict a relatively narrow ($\Gamma \sim 0.11$ MeV) 2_1^+ state at $E_T \sim 1.6$ MeV. The right “wing” of this peak could be situated on a “background” formed by 0_2^+ and, maybe, 0_3^+ states.

Evidence for the ^{26}O excited state at about $E_T = 4.2$ MeV was obtained in Ref. [4], although with marginal statistics. Within this energy range we predict quite broad and overlapping 2_2^+ and 0_4^+ states.

X. CONCLUSIONS

We studied the 0^+ and 2^+ continuum properties of the ^{26}O system in three-cluster $^{24}\text{O}+n+n$ theoretical model. The main results obtained in this work are:

(i) The ground state decay spectrum of the long-living $2n$ emitters can be very well approximated in a broad energy range by a simple analytical expression generalizing R -matrix phenomenology for use in the hyperspherical space of three-body systems.

(ii) A number of monopole (breathing mode) excited 0^+ states are predicted in ^{26}O at about 1.76, 2.6, and 4.2 MeV. These states extend to extreme distances in radial space with typical single-particle orbital sizes around 20 fm. The predicted densely spaced sequence of 0^+ states in the ^{26}O continuum states with such radial properties resembles the Efimov phenomenon. These states can probably be considered as the lowest Efimov states forced into continuum by insufficient binding.

(iii) The predicted 2^+ states in ^{26}O at 1.6 and 4.5 MeV are in a reasonable agreement with continuum shell model calculations.

(iv) We suggest to identify the experimentally observed intensity in the range of 1–2 MeV in the spectrum of ^{26}O as a “pile up” of 0_2^+ and 2_1^+ state contributions. The possible experimental peak at ~ 4 MeV in ^{26}O can be associated with overlapping broad 2_2^+ and 0_3^+ continuum states.

ACKNOWLEDGMENTS

We are grateful to Prof. G. Nyman for a careful reading of the manuscript and numerous useful comments. L.V.G. is partly supported by Russian Foundation for Basic Research Grant No. 14-02-00090-a and Ministry of Education and Science of the Russian Federation Grant No. NSh-932.2014.2.

[1] C. R. Hoffman, T. Baumann, D. Bazin, J. Brown, G. Christian, P. A. DeYoung, J. E. Finck, N. Frank, J. Hinnefeld, R. Howes *et al.*, *Phys. Rev. Lett.* **100**, 152502 (2008).
 [2] E. Lunderberg, P. A. DeYoung, Z. Kohley, H. Attanayake, T. Baumann, D. Bazin, G. Christian, D. Divaratne, S. M. Grimes, A. Haagsma *et al.*, *Phys. Rev. Lett.* **108**, 142503 (2012).
 [3] Z. Kohley, T. Baumann, D. Bazin, G. Christian, P. A. DeYoung, J. E. Finck, N. Frank, M. Jones, E. Lunderberg, B. Luther *et al.*, *Phys. Rev. Lett.* **110**, 152501 (2013).

[4] C. Caesar, J. Simonis, T. Adachi, Y. Aksyutina, J. Alcantara, S. Altstadt, H. Alvarez-Pol, N. Ashwood, T. Aumann, V. Avdeichikov *et al.* (R3B Collaboration), *Phys. Rev. C* **88**, 034313 (2013).
 [5] Y. Kondo, T. Nakamura, N. L. Achouri, T. Aumann, H. Baba, F. Delaunay, P. Doornenbal, N. Fukuda, J. Gibelin, J. Hwang *et al.*, Proceedings of the 2nd International Conference on the Advance in Radioactive Isotope Science (ARIS2014), JPS Conf. Proc. (2014) (unpublished).

- [6] A. Volya and V. Zelevinsky, *Phys. Rev. C* **74**, 064314 (2006).
- [7] G. Hagen, T. Papenbrock, D. J. Dean, M. Hjorth-Jensen, and B. Velamuri Asokan, *Phys. Rev. C* **80**, 021306(R) (2009).
- [8] T. Otsuka, T. Suzuki, J. D. Holt, A. Schwenk, and Y. Akaishi, *Phys. Rev. Lett.* **105**, 032501 (2010).
- [9] H. Hergert, S. Binder, A. Calci, J. Langhammer, and R. Roth, *Phys. Rev. Lett.* **110**, 242501 (2013).
- [10] L. V. Grigorenko, I. G. Mukha, C. Scheidenberger, and M. V. Zhukov, *Phys. Rev. C* **84**, 021303(R) (2011).
- [11] L. V. Grigorenko, I. G. Mukha, and M. V. Zhukov, *Phys. Rev. Lett.* **111**, 042501 (2013).
- [12] K. Hagino and H. Sagawa, *Phys. Rev. C* **89**, 014331 (2014).
- [13] K. Hagino and H. Sagawa, *Phys. Rev. C* **90**, 027303 (2014).
- [14] L. V. Grigorenko, T. D. Wisner, K. Miernik, R. J. Charity, M. Pfützner, A. Banu, C. R. Bingham, M. Cwiok, I. G. Darby, W. Dominik *et al.*, *Phys. Lett. B* **677**, 30 (2009).
- [15] L. V. Grigorenko, T. D. Wisner, K. Mercurio, R. J. Charity, R. Shane, L. G. Sobotka, J. M. Elson, A. H. Wuosmaa, A. Banu, M. McCleskey *et al.*, *Phys. Rev. C* **80**, 034602 (2009).
- [16] I. A. Egorova, R. J. Charity, L. V. Grigorenko, Z. Chajecki, D. Coupland, J. M. Elson, T. K. Ghosh, M. E. Howard, H. Iwasaki, M. Kilburn *et al.*, *Phys. Rev. Lett.* **109**, 202502 (2012).
- [17] L. V. Grigorenko, I. A. Egorova, R. J. Charity, and M. V. Zhukov, *Phys. Rev. C* **86**, 061602(R) (2012).
- [18] A. Fomichev, V. Chudoba, I. Egorova, S. Ershov, M. Golovkov, A. Gorshkov, V. Gorshkov, L. Grigorenko, G. Kamiski, S. Krupko *et al.*, *Phys. Lett. B* **708**, 6 (2012).
- [19] B. V. Danilin, M. V. Zhukov, S. N. Ershov, F. A. Gareev, R. S. Kurmanov, J. S. Vaagen, and J. M. Bang, *Phys. Rev. C* **43**, 2835 (1991).
- [20] J. Bang, B. Danilin, V. Efros, J. Vaagen, M. Zhukov, and I. Thompson, *Phys. Rep.* **264**, 27 (1996).
- [21] B. V. Danilin, J. S. Vaagen, T. Rogde, S. N. Ershov, I. J. Thompson, and M. V. Zhukov (RNBT Collaboration), *Phys. Rev. C* **76**, 064612 (2007).
- [22] S. Ershov and B. Danilin, *Phys. Part. Nucl.* **39**, 835 (2008).
- [23] S. Ershov and B. Danilin, *Phys. At. Nucl.* **72**, 1704 (2009).
- [24] K. W. Brown, R. J. Charity, L. G. Sobotka, Z. Chajecki, L. V. Grigorenko, I. A. Egorova, Y. L. Parfenova, M. V. Zhukov, S. Bedoor, W. W. Buhro *et al.*, *Phys. Rev. Lett.* **113**, 232501 (2014).
- [25] L. V. Grigorenko, T. A. Golubkova, and M. V. Zhukov, *Phys. Rev. C* **91**, 024325 (2015).
- [26] L. V. Grigorenko, B. V. Danilin, V. D. Efros, N. B. Shul'gina, and M. V. Zhukov, *Phys. Rev. C* **57**, R2099 (1998).
- [27] L. V. Grigorenko, R. C. Johnson, I. G. Mukha, I. J. Thompson, and M. V. Zhukov, *Phys. Rev. C* **64**, 054002 (2001).
- [28] L. V. Grigorenko and M. V. Zhukov, *Phys. Rev. C* **77**, 034611 (2008).
- [29] P. G. Sharov, I. A. Egorova, and L. V. Grigorenko, *Phys. Rev. C* **90**, 024610 (2014).
- [30] D. Gogny, P. Pires, and R. D. Tournier, *Phys. Lett. B* **32**, 591 (1970).
- [31] M. Pfützner, M. Karny, L. V. Grigorenko, and K. Riisager, *Rev. Mod. Phys.* **84**, 567 (2012).
- [32] M. S. Golovkov, L. V. Grigorenko, A. S. Fomichev, Y. T. Oganessian, Y. I. Orlov, A. M. Rodin, S. I. Sidorchuk, R. S. Slepnev, S. V. Stepantsov, G. M. Ter-Akopian *et al.*, *Phys. Lett. B* **588**, 163 (2004).
- [33] S. K. Bogner, H. Hergert, J. D. Holt, A. Schwenk, S. Binder, A. Calci, J. Langhammer, and R. Roth, *Phys. Rev. Lett.* **113**, 142501 (2014).